

# Possible ferrimagnetism and ferroelectricity of half-substituted rare-earth titanate: A first-principles study on $Y_{0.5}La_{0.5}TiO_3$

Ming An, Hui-Min Zhang, Ya-Kui Weng, Yang Zhang, Shuai Dong<sup>†</sup>

Department of Physics, Southeast University, Nanjing 211189, China

Corresponding author. E-mail: <sup>†</sup>sdong@seu.edu.cn

Received November 3, 2015; accepted November 26, 2015

Titanates with the perovskite structure, including ferroelectrics (e.g.,  $BaTiO_3$ ) and ferromagnetic ones (e.g.,  $YTiO_3$ ), are important functional materials. Recent theoretical studies predicted multi-ferroic states in strained  $EuTiO_3$  and titanate superlattices, the former of which has already been experimental confirmed. Here, a first-principles calculation is performed to investigate the structural, magnetic, and electronic properties of Y half-substituted  $LaTiO_3$ . Our results reveal that the magnetism of  $Y_{0.5}La_{0.5}TiO_3$  sensitively depends on its structural details because of the inherent phase competition. The lowest energy state is the ferromagnetic state, resulting in  $0.25 \mu_B/Ti$ . Furthermore, some configurations of  $Y_{0.5}La_{0.5}TiO_3$  exhibit hybrid improper polarizations, which can be significantly affected by magnetism, resulting in the multiferroic properties. Because of the quenching disorder of substitution, the real  $Y_{0.5}La_{0.5}TiO_3$  material with random A-site ions may exhibit interesting relaxor behaviors.

**Keywords** titanate, ferrimagnetic, ferroelectricity

**PACS numbers** 75.85.+t, 77.84.Cg, 75.50.Gg

## 1 Introduction

Strongly correlated electron materials in the form of transition metal oxides exhibit many fascinating physical phenomena, e.g., high- $T_c$  superconductivity, colossal magnetoresistivity, and multiferroicity, which have attracted significant research attention [1]. Among various oxides, titanium oxides (titanates) with pseudo-cubic perovskite structures (with a uniform chemical formula of  $ATiO_3$  or  $RTiO_3$ ) possess some peculiar physical properties. In titanates, there are multiple ferroic phases, covering ferromagnetic (FM), antiferromagnetic (AFM), ferroelectric (FE), quantum paraelectric, and even hybrids of these orders. More notably, a recent theoretical study predicted strained  $EuTiO_3$  to be FM and FE [2], a rare but desired multiferroic property, which was later experimentally confirmed [3]. In addition, an orbital-ordering-driven insulating phase was predicted in the  $LaTiO_3/SrTiO_3$  superlattice, which exhibited ferrimagnetism and ferroelectricity [4]. These pioneering works provide a promising perspective of titanates to pursue desired functional properties using careful designs.

Physically, the properties of perovskite titanates depend on the valence of the A-site cations. For the di-

valent  $A^{2+}$ ,  $Ti^{4+}$  is usually FE-active, which can cause an appropriate FE polarization, as in  $BaTiO_3$ . In contrast, for trivalent  $R^{3+}$  (mostly rare earth), the  $Ti^{3+}$  is magnetic, with  $1 \mu_B/Ti$  moment. The magnetic ground state depends on the size of  $R^{3+}$  because of the coupling between the structural-orbital-magnetic degrees of freedom [5–8]. In particular, the G-type AFM (G-AFM) order appears for large  $R^{3+}$  (e.g.,  $La^{3+}$ ) [5, 7], whereas the FM phase is stable when  $R^{3+}$  is small (e.g.,  $Y^{3+}$ ) [5, 6], as illustrated in Fig. 1(b). This magnetic phase diagram as a function of  $R^{3+}$  is somewhat similar to that of  $RMnO_3$  [9], both of which are full of phase competition, although the detail phases are not identical.

In the present work, we will study  $Y_{0.5}La_{0.5}TiO_3$ , namely half-Y-substituted  $LaTiO_3$  or vice versa. There are two purposes of this study. First, using our abundant experience on manganites, we propose that the ionic substitution may generate emergent phases, which are different from the phases of the parents [9]. Thus, we question whether there are any novel new phases hidden in the titanate family. Second, following the recent prediction based on the  $LaTiO_3/SrTiO_3$  superlattice [4], we want to determine whether it is possible to achieve a multiferroic state in more titanates. In particular, charge-orbital-ordering, a crucial part of the  $LaTiO_3/SrTiO_3$

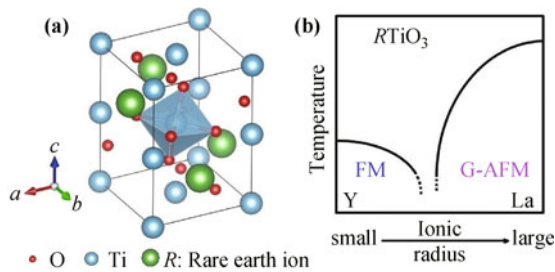


**Fig. 1** (a) Schematic structure of  $RTiO_3$  unit cell. (b) Schematic phase diagram of  $RTiO_3$  family.

superlattice [4], is a sensitive physical property, which requires appropriate electronic correlation and special lattice distortions. Is there any alternative selection to avoid these sensitive conditions and pursue multiferroicity in an easier manner? In our study, because  $La^{3+}$  and  $Y^{3+}$  are isovalent, no charge ordering is involved in the  $Y_{0.5}La_{0.5}TiO_3$ , leaving a robust Mott insulator with single-valent  $Ti^{3+}$ .

## 2 Model and method

Bulk  $LaTiO_3$  has an orthorhombic structure (space group  $Pbnm$ ) with experimental lattice parameters of  $a=5.636$  Å,  $b=5.618$  Å, and  $c=7.916$  Å [10], as shown in Fig. 1(a).  $YTiO_3$  has an identical structure to that of  $LaTiO_3$  but with slightly different lattice constants, i.e.,  $a=5.338$  Å,  $b=5.690$  Å, and  $c=7.613$  Å [11]. Although they share the same space group, these two titanates have different magnetic ground states because of the different magnitudes of the  $GdFeO_3$ -type distortions [2]. According to a previous study,  $LaTiO_3$  exhibits the G-AFM order below 146 K, whereas the more-distorted  $YTiO_3$  exhibits ferromagnetism below 30 K [5].

Our first-principles calculations are performed using

the projector augmented wave approach as implemented in the Vienna *ab initio* simulation package (VASP) [12, 13]. The electronic correlation is treated in terms of the generalized gradient approximation (GGA) [14] with Hubbard  $U$  imposed on Ti  $d$  states, which is set as  $U_{eff} = U - J = 3.2$  eV [6–8], using the Dudarev implementation [15]. The optimization and electronic self-consistent interactions are performed using a plane-wave cut-off of 500 eV and a  $\Gamma$ -centered Monkhorst–Pack  $k$ -point mesh of  $7 \times 7 \times 5$ . Both the lattice constants and inner atomic positions are fully optimized as the Hellman–Feynman forces converge to within 10 meV/Å. These parameters are standard choices and have been demonstrated to yield good agreement with experimental data [6–8]. The standard Berry phase method is employed to calculate the FE polarization [16].

## 3 Results and discussion

As a benchmark test, the crystal and magnetic structures of the parent compound  $LaTiO_3$  are determined. First, the fully relaxed lattice of the nonmagnetic state gives  $a=5.714$  Å,  $b=5.687$  Å, and  $c=8.003$  Å, which are close to the aforementioned experimental values. The slight overestimation of the structural size is common when using GGA. Then, four magnetic states, FM, A-type AFM (A-AFM), C-type AFM (C-AFM), and G-AFM, are applied. By comparing their energies, it is demonstrated that the G-type AFM is the most stable state, which is consistent with experimental results. In addition,  $YTiO_3$  was tested in our previous work [6]. These tests provide a good starting point to continue the following structural relaxation, magnetism, and polarization calculations on  $Y_{0.5}La_{0.5}TiO_3$ .

In our study, the Y-substitution is performed in the

**Table 1** The relaxed lattice structure of  $Y_{0.5}La_{0.5}TiO_3$  in three configurations with and without magnetism. Symmetry groups of those structures are also listed here.

	A		B		C	
Relaxed lattice constants (Å)	Nonmagnetic	Ferrimagnetic	Nonmagnetic	A-AFM	Nonmagnetic	Ferrimagnetic
	$a = 5.580$	$a = 5.552$	$a = 5.536$	$a = 5.531$	$a = 5.567$	$a = 5.550$
	$b = 5.710$	$b = 5.841$	$b = 5.719$	$b = 5.806$	$b = 5.714$	$b = 5.794$
	$c = 7.857$	$c = 7.850$	$c = 7.875$	$c = 7.924$	$c = 7.867$	$c = 7.925$
Volume (Å <sup>3</sup> )	250.347	254.575	249.336	254.430	250.226	254.750
Space group	$Pmn2_1$		$Pmc2_1$		$P2_1/m$	
Point group	$mm2$		$mm2$		$2/m$	

minimal unit cell, which contains four chemical units (i.e., four Ti's). Then, for the half-substituted case, there are three independent configurations (denoted as A: rock salt, B: layered, and C: columnar [17]), as listed in Table 1. The structures for these three configurations are fully optimized. The relaxed structures (without magnetism) are slightly different from each other, as summarized in Table 1. According to symmetry analysis, the lattice structures of configurations A and B are associated with polar point group  $mm2$ , whereas C is associated with the centrosymmetric point group  $2/m$ .

Subsequently, the spin-polarized calculations are performed. Both the lattice framework and internal atomic positions are further relaxed with various magnetic orders. The total energies for all the independent configurations are obtained and compared, as shown in Fig. 2(a). Not only are the aforementioned FM and multiple AFM states considered, two ferrimagnetic orders [insert of Fig. 2(a)] are also considered considering the lowered symmetry induced by substitutions.

As shown in Fig. 2(a), among the three configurations, configuration A has the lowest energy despite the details

of the magnetic orders. More notably, the ferrimagnetic state with the  $\uparrow\downarrow\uparrow\uparrow$  spin configuration has the lowest energy for both A and C, whereas the A-AFM state is the most stable state for B (the energy of the FM state is only slightly higher). Thus, the magnetic ground state sensitively depends on the structural details, i.e., the Y-La configuration. In addition, the ferrimagnetic state is quite novel because it does not exist in the phase diagram of unsubstituted  $RTiO_3$ . According to the energy difference between the lowest energy magnetic state and nonmagnetic state, the ferrimagnetic transition temperature of configuration A can be roughly estimated as  $\sim 43$  K, with the references of pure  $YTiO_3$  and  $LaTiO_3$ .

This sensibility of magnetism can be reasonably understood considering the phase diagram of  $RTiO_3$ . There is a strong tendency of inherent phase competition, which is closely related to the orbital ordering associated with the structural distortions [5–8]. In  $Y_{0.5}La_{0.5}TiO_3$ , the distortions are modulated from two aspects: i) the lattice constants  $a$ - $b$ - $c$  are compromises between those of  $LaTiO_3$  and  $YTiO_3$ , making the system close to the phase boundary and; ii) the local  $TiO_6$  octahedron is also tuned, generating multiple values for bond length/angle even within the minimal unit, as illustrated in Figs. 2(b) and (c). The second point may further frustrate magnetic exchanges.

The competition between FM and AFM Ti-O-Ti exchanges is determined by the bond structure (length and angle). The underlying driving force is the orbital ordering. Previous theoretical studies have demonstrated that the ferromagnetism of  $YTiO_3$  is accompanied by a particular orbital order, which is stabilized by  $t_{2g}$ - $e_g$  hybridization induced by the  $GdFeO_3$ -type distortion [5]. On one hand, considering the  $GdFeO_3$ -type distortion, the Y substitution should indeed strengthen the FM tendency in competition. The averaged bond lengths and bond angles of  $Y_{0.5}La_{0.5}TiO_3$  are between the original values of the parents,  $LaTiO_3$  and  $YTiO_3$ , as illustrated in Figs. 2(b) and (c). On the other hand, the substitution causes anisotropic deformation to  $TiO_6$  octahedra, causing the bond lengths and bond angles to bifurcate [also depicted in Figs. 2(b) and (c)]. With different bond lengths/angles, the exchanges determined by the orbital ordering become nonuniform in the system, e.g., resulting in some FM and some AFM exchanges. Thus, the ferrimagnetic state, as a hybrid state between the full FM and full AFM states, emerges in the substituted system.

In summary, with magnetism,  $Y_{0.5}La_{0.5}TiO_3$  likely exhibits a net magnetic moment as a result of the ferrimagnetism. The calculated moment is  $1 \mu_B/u.c.$  ( $0.25 \mu_B/Ti$ ) for the ideal ferrimagnetic state. Moreover, according to above symmetry analysis in Table 1, the sub-

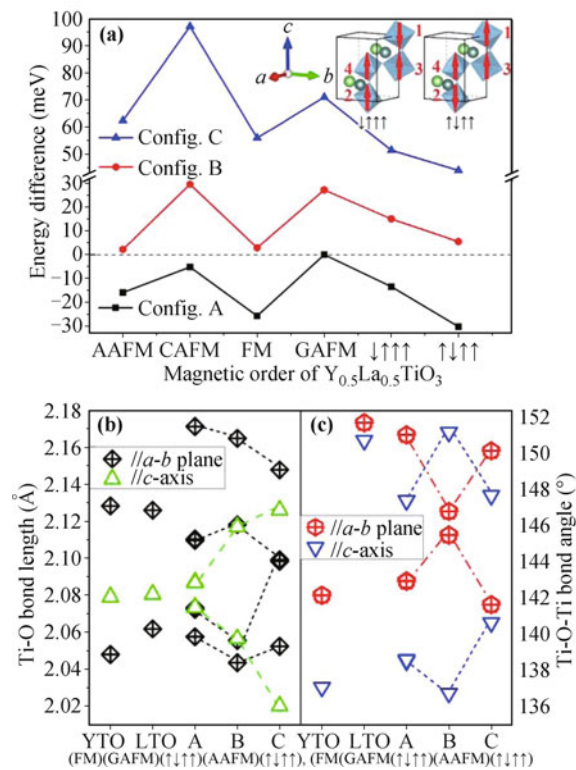


**Fig. 2** (a) The total energy of  $Y_{0.5}La_{0.5}TiO_3$  in three configurations (A, B, and C) as a function of different magnetic orders including AFM, C-AFM, FM, G-AFM, and two types of ferrimagnetism denoted as  $\uparrow\uparrow\uparrow$  and  $\uparrow\downarrow\uparrow$ . The total energies shown here refer to the value of G-AFM state of configuration A for a minimal unit cell (20 atoms) (b) Ti-O bond lengths and (c) Ti-O-Ti bond angles inside and outside  $ab$ -plane of local  $TiO_6$  octahedron in optimized structures with stablest magnetism.

stitution can break the space inversion symmetry for configurations A and B, at least on the unit cell scale, which can lead to local electric dipoles. To confirm this point, standard Berry phase calculations were performed, and the results are summarized in Table 2. The centrosymmetric phase (e.g., configuration C) is adopted as the reference state in the Berry phase calculation. It is clear that moderate polarizations indeed exist for cases A and B, whereas C is non-polar.

The origin of polarization can be understood as hybrid improper ferroelectricity, which was first proposed for  $\text{PbTiO}_3/\text{SrTiO}_3$  superlattices [18] and then extended to other superlattices and bulks [19–21]. In our study, all three configurations can be considered as special superlattices stacking along different directions [22]. For example, viewed from an appropriate direction (Fig. 3), cases A and B equal the superlattices with layered modulation of A-site cations. Previous studies have confirmed that the modulation of non-polar antiferroelectric distortions (AFD) in  $(\text{ABO}_3)_1/(\text{A}'\text{BO}_3)_1$  superlattices oriented along the [001] axis can cause an in-plane FE polarization [23]. Our case B just mimics the [001]-orientated superlattice, whereas case A can be considered as the pseudocubic [111]-oriented (the [101] in the  $Pbnm$  notation) superlattice. Both of these two cases are polar. In contrast, the case C is in analog to the pseudocubic [110]-orientated (the [100] in the  $Pbnm$  notation) superlattice, which is non-polar according to the symmetry. In this sense, the hybrid improper ferroelectricity predicted in our study is derived from additional lattice distortions induced by mismatch of the different A-site cations. Such a geometric ferroelectricity can usually persist to a high temperature above room temperature [18–21].

Although here, the polarization is mainly from the structural distortions, the magnetism can still significantly affect the polarization. As observed in Table 2, the polarization changes significantly from the non-magnetic to magnetic ground state. An FM transition, e.g., under a strong enough magnetic field, can further

**Table 2** The ferroelectric polarization of  $\text{Y}_{0.5}\text{La}_{0.5}\text{TiO}_3$  calculated using the Berry phase method. For each configuration, three types of structures are adopted: i) nonmagnetic optimized structure; ii) the stablest magnetic relaxed structure, and iii) ferromagnetic optimized structure. The difference between these values is due to the magnetic striction effect.

Configuration		A	B	C
Nonmagnetic	Polarization ( $\mu\text{C}/\text{cm}^2$ )	4.02	7.01	0
	Direction	[100]	[010]	/
Stablest magnetic	Polarization ( $\mu\text{C}/\text{cm}^2$ )	1.70	2.64	0
	Direction	[100]	[010]	/
Ferromagnetic	Polarization ( $\mu\text{C}/\text{cm}^2$ )	0.23	2.47	0
	Direction	[100]	[010]	/

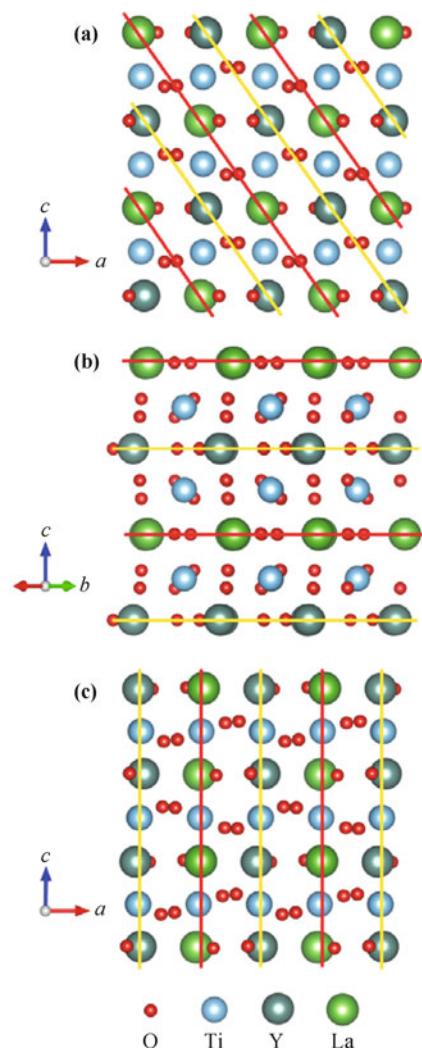


**Fig. 3** The superlattice-like structures of  $\text{Y}_{0.5}\text{La}_{0.5}\text{TiO}_3$ . (a) For the configuration A, it is stacked along the [101] axis in  $Pbnm$  notation (or the [111] axis in pseudocubic framework). (b) For the configuration B, it is along the [001] direction. (c) For the configuration C, it is along the [100] axis in  $Pbnm$  notation (or the [110] axis in pseudocubic framework).

suppress the polarization. Especially for configuration A, the suppression can be up to 86% of the ferrimagnetic one, rendering a promising magnetoelectric effect. Therefore, it is possible to control the ferroelectricity using an applied magnetic field even though the directions of polarizations are not changed upon magnetism. In addition, because of the coexistence of spontaneous polarization and magnetization in the current system, the magnetoelectric response should not be simply linear.

Considering the real compounds, the substituted ions will not be therefore ideally ordered as the three configurations studied in our simulation, which should be distributed partially and randomly. Thus, the inhomogeneity should exist anywhere in the sample because of this quenching disorder, even though configuration A

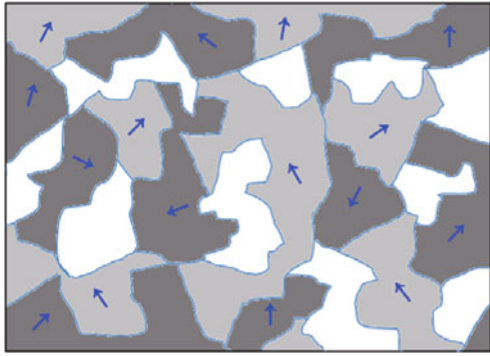


**Fig. 4** Schematic of real compounds with three configurations distributed randomly in nano-scale. Here three types of “domains” (corresponding to the three configurations studied in the present work) are shown although there may exist more possible configurations, some of which possess ferrimagnetism and/or ferroelectricity as indicated by arrows. These local magnetic moments and ferroelectric dipoles can be magnetized and polarized by external magnetic and electric fields, respectively.

is most energetically preferred. Considering the insulating behavior (no itinerant electrons/holes), the physical properties of the real material will reflect averaged effects of all three of these structures as well as other possible configurations, as sketched in Fig. 4. In this sense, the net magnetization remains expectable considering the ferrimagnetism (cases A and C). In addition, because of the random orientation of electric polarization inside nanoclusters, the net component may be weak. However, the local dipole moments, if polished by electric fields, can cause a finite polarization. Because of the inhomogeneity, the critical temperatures for magnetic transition and FE transition may be broad in two ranges, instead of two points, as in relaxor FEs [24]. In addition, glassy-like magnetic and FE behaviors may exist, as observed in phase-separated manganites.

## 4 Summary

In summary, the lattice, magnetic, and electronic structure of Y half-substituted  $\text{LaTiO}_3$  were studied using the GGA+ $U$  method. The magnetic ground state sensitively depended on the structural distortion induced by substitution and consists of probable ferrimagnetism with a moderate net spin moment. In addition, the ferroelectricity was predicted from symmetry analysis and confirmed by the calculation. This polarization can be observed as hybrid improper ferroelectricity and can be modulated by magnetism, showing a promising magnetoelectric effect. Our work provides a simple route to realize multiferroicity in titanates.

**Acknowledgements** This work was supported by the National

Natural Science Foundation of China (Grant Nos. 11274060 and 51322206).

## References and notes

1. E. Dagotto, Complexity in strongly correlated electronic systems, *Science* 309(5732), 257 (2005)
2. C. J. Fennie and K. M. Rabe, Magnetic and electric phase control in epitaxial  $\text{EuTiO}_3$  from first principles, *Phys. Rev. Lett.* 97(26), 267602 (2006)
3. J. H. Lee, L. Fang, E. Vlahos, X. L. Ke, Y. W. Jung, L. F. Kourkoutis, J. W. Kim, P. J. Ryan, T. Heeg, M. Roeckerath, V. Goian, M. Bernhagen, R. Uecker, P. C. Hammel, K. M. Rabe, S. Kamba, J. Schubert, J. W. Freeland, D. A. Muller, C. J. Fennie, P. Schiffer, V. Gopalan, E. Johnston-Halperin, and D. G. Schlom, A strong ferroelectric ferromagnet created by means of spin–lattice coupling, *Nature* 466(7309), 954 (2010)
4. N. C. Bristowe, J. Varignon, D. Fontaine, E. Bousquet, and P. Ghosez, Ferromagnetism induced by entangled charge and orbital orderings in ferroelectric titanate perovskites, *Nat. Commun.* 6, 6677 (2015)
5. M. Mochizuki and M. Imada, Orbital physics in the perovskite Ti oxides, *New J. Phys.* 6, 154 (2004)
6. X. Huang, Y. Tang, and S. Dong, Strain-engineered A-type antiferromagnetic order in  $\text{YTiO}_3$ : A first-principles calculation, *J. Appl. Phys.* 113, 17E108 (2013)
7. Y. Weng, X. Huang, and S. Dong, Magnetic orders of  $\text{LaTiO}_3$  under epitaxial strain: A first-principles study, *J. Appl. Phys.* 115, 17E108 (2014)
8. L. Yang, Y. Weng, H. Zhang, and S. Dong, Strain driven sequential magnetic transitions in strained  $\text{GdTiO}_3$  on compressive substrates: A first-principles study, *J. Phys.: Condens. Matter* 26(47), 476001 (2014)
9. S. Dong, R. Yu, S. Yunoki, J. M. Liu, and E. Dagotto, Origin of multiferroic spiral spin order in the  $\text{RMnO}_3$  perovskites, *Phys. Rev. B* 78(15), 155121 (2008)
10. A. C. Komarek, H. Roth, M. Cwik, W. D. Stein, J. Baier, M. Kriener, F. Bouree, T. Lorenz, and M. Braden, Magnetoelastic coupling in  $\text{RTiO}_3$  (R=La, Nd, Sm, Gd, Y) investigated with diffraction techniques and thermal expansion measurements, *Phys. Rev. B* 75(22), 224402 (2007)
11. M. Cwik, T. Lorenz, J. Baier, R. Muller, G. Andre, F. Bouree, F. Lichtenberg, A. Freimuth, R. Schmitz, E. Muller-Hartmann, and M. Braden, Crystal and magnetic structure of  $\text{LaTiO}_3$ : Evidence for non-degenerate  $t_{2g}$ -orbitals, *Phys. Rev. B* 68(6), 060401 (2003)
12. G. Kresse and J. Hafner, Ab initio molecular dynamics for liquid metals, *Phys. Rev. B* 47(1), 558 (1993)
13. G. Kresse and J. Furthmuller, Efficient iterative schemes for *ab initio* total-energy calculations using a plane-wave basis set, *Phys. Rev. B* 54(16), 11169 (1996)

14. J. P. Perdew, K. Burke, and M. Ernzerhof, Generalized gradient approximation made simple, *Phys. Rev. Lett.* 77(18), 3865 (1996)
15. S. L. Dudarev, G. A. Botton, S. Y. Savrasov, C. J. Humphreys, and A. P. Sutton, Electron-energy-loss spectra and the structural stability of nickel oxide: A LSDA+*U* study, *Phys. Rev. B* 57(3), 1505 (1998)
16. R. D. King-Smith and D. Vanderbilt, Theory of polarization of crystalline solids, *Phys. Rev. B* 47(3), 1651 (1993)
17. J. Young and J. M. Rondinelli, Atomic scale design of polar perovskite oxides without second-order Jahn–Teller ions, *Chem. Mater.* 25(22), 4545 (2013)
18. E. Bousquet, M. Dawber, N. Stucki, C. Lichtensteiger, P. Hermet, S. Gariglio, J. M. Triscone, and P. Ghosez, Improper ferroelectricity in perovskite oxide artificial superlattices, *Nature* 452(7188), 732 (2008)
19. N. A. Benedek and C. J. Fennie, Hybrid improper ferroelectricity: A mechanism for controllable polarization-magnetization coupling, *Phys. Rev. Lett.* 106(10), 107204 (2011)
20. H. M. Zhang, Y. K. Weng, X. Y. Yao, and S. Dong, Charge transfer and hybrid ferroelectricity in  $(\text{YFeO}_3)_n/(\text{YTlO}_3)_n$  magnetic superlattices, *Phys. Rev. B* 91(19), 195145 (2015)
21. J. Alaria, P. Borisov, M. S. Dyer, T. D. Manning, S. Lepadatu, M. G. Cain, E. D. Mishina, N. E. Sherstyuk, N. A. Ilyin, J. Hadermann, D. Lederman, J. B. Claridge, and M. J. Rosseinsky, Engineered spatial inversion symmetry breaking in an oxide heterostructure built from isosymmetric room-temperature magnetically ordered components, *Chem. Sci.* 5(4), 1599 (2014)
22. H. M. Zhang, M. An, X. Y. Yao, and S. Dong, Orientation-dependent ferroelectricity of strained  $\text{PbTiO}_3$  films, *Front. Phys.* 10(5), 107701 (2015)
23. J. M. Rondinelli and C. J. Fennie, Octahedral rotation-induced ferroelectricity in cation ordered perovskites, *Adv. Mater.* 24(15), 1961 (2012)
24. D. V. B. Murthy and G. Srinivasan, Broadband ferromagnetic resonance studies on influence of interface bonding on magnetoelectric effects in ferrite–ferroelectric composites, *Front. Phys.* 7, 418 (2012)